

## Radiation Spectra of Advection Dominated Accretion Flows around Kerr Black Holes

by

A. Kurpiewski and M. Jaroszyński

Warsaw University Observatory, Al. Ujazdowskie 4, 00-478 Warszawa,  
e-mail: kurpiew@astrouw.edu.pl, mj@astrouw.edu.pl

*Received 2000*

### ABSTRACT

We study the formation of the spectra in advection dominated accretion flows (ADAFs) around Kerr black holes. We use a Monte Carlo approach and fully general relativistic treatment to follow the paths of individual photons and model their scattering with mildly relativistic, thermal electrons of the two temperature plasma present in the flow. We study the influence of the accretion rate, black hole mass, black hole angular momentum, and the strength of the small scale magnetic field present in the plasma on the resulting spectra. The impact of the black hole angular momentum on the spectra is present and can be distinguished from the influence of changes in other parameters. This property of the models should be taken into account when modeling the individual sources and the population of inefficiently accreting black holes in the Universe.

**Key words:** *black holes - accretion - radiation processes*

### 1. Introduction

The Advection Dominated Accretion Flows (ADAFs) have been reviewed by a number of authors, most recently by Yi (1999), Lasota (1999), Narayan, Mahadevan and Quataert (1998), Svensson (1998), and Kato, Fukue and Mineshige (1998). The ADAFs represent a class of optically thin solutions of the accretion flow, which radiate so inefficiently, that almost all the heat dissipated inside the fluid is subsequently advected toward the black hole horizon. Since the cooling of matter is negligible, the equations of fluid dynamics are independent of the equations describing the emission, absorption and scattering of radiation. This allows one to address these two topics separately. In this paper we are concerned mostly with the radiation processes inside the flow.

The fully relativistic dynamics of ADAFs has been described and some solutions have been obtained in Lasota (1994), Abramowicz et al. (1996), Abramowicz,

Lanza and Percival (1997), Peitz and Appl (1997), Jaroszyński and Kurpiewski (1997, hereafter Paper I), Gammie and Popham (1998), and Popham and Gammie (1998). The most extensive survey of the parameter space is probably presented by Popham and Gammie (1998), where the dependence of the flow on the black hole spin defined by the dimensionless Kerr parameter  $a$ , the viscosity parameter  $\alpha$ , the gas adiabatic index, and on the advection parameter  $f$  (where  $f = 1$  means fully advective flow without any cooling) is investigated. This work shows rather strong dependence of the flow characteristics on parameters mentioned, especially on the black hole spin. The dependence on advection parameter is also substantial, but for a narrow range of  $f$ , which can represent flows with negligible cooling ( $0.9 \leq f \leq 1$ ) one can use the  $f = 1$  solutions.

In our calculations we use the solutions of the equations describing the flow dynamics presented in Paper I. All our models use  $f = 1$ , which is representative of the physically relevant ADAFs. The black hole spin, we consider, is limited to the three values ( $a = 0, 0.5$ , and  $0.9$ ). We also use only one value of the viscosity parameter  $\alpha = 0.1$ .

The main purpose of this paper is a self-consistent treatment of photon Comptonization in a two temperature plasma of an ADAF solution and a limited survey of the parameter space of the models. We check the dependence of the resulting spectra on the black hole mass and spin, accretion rate, and the parameter describing the importance of the small scale magnetic fields  $\beta$ .

In our previous paper on the subject (Kurpiewski and Jaroszyński 1999, hereafter Paper II) we have described the methods of calculating the spectra of ADAFs using Monte Carlo approach to follow the individual photons and taking into account all the relativistic effects in photon propagation. We use this approach here with two changes: following Nakamura et al. (1997) and Narayan et al. (1998, hereafter NMGP) we modify the thermal balance equation adding terms describing viscous heating of the electrons and advection of heat by them.

In the next Section we present the modifications of the methods employed in Papers I and II. In Sec. 3 we present the results of calculations, showing some details of the structure of the various ADAF configurations and the spectra produced by them. The discussion and conclusions follow in the last Section.

## 2. The model

The dynamics of the flow, the methods of calculating the cooling rate at a chosen location in the configuration when the density and electron temperature are given, as well as the Monte Carlo approach to Comptonization are fully described in Papers I and II. We are not going to repeat it here. The only substantial change in our methods compared to the previous papers is the new treatment of the thermal equilibrium in the two temperature plasma. Following Nakamura et al. (1997) and NMGP we calculate the amount of heat advected by the electron gas. This factor

is unimportant in the energy budget of the whole configuration but may be important in finding the temperature of the electrons. We also include the possibility that the electrons gain some thermal energy directly from the dissipative processes. Both processes influence the electron thermal energy balance. Such terms have been usually neglected under the assumption that the equilibrium between Coulomb heating and various cooling processes for electrons is quickly established.

Our models are obtained under many simplifying assumptions. In particular we solve the equations for the “vertically averaged, stationary configuration” (Abramowicz et al. 1996; Narayan and Yi 1994) which is a standard procedure in ADAFs. We make also some more detailed assumptions postulating that in the spherical coordinate system (Boyer Lindquist coordinates, see Bardeen 1973) the fluid has no poloidal velocity component. We also assume that the speed of sound, the radial velocity component, and the specific angular momentum of the fluid depend only on the radial coordinate. These assumptions are sufficient to fully describe the pressure and density distribution in three dimensional configuration (see Paper II). The distribution of electron temperature needs further treatment which we describe with some details below.

The thermodynamics of the gas and magnetic field is described by the set of equations given by NMGP. We only introduce some factors which one may treat as relativistic corrections.

In ADAF models which use synchrotron radiation as a source of soft photons it is usually assumed that the ratio of the magnetic pressure to the gas pressure is constant ( $P_m/P_g = (1 - \beta)/\beta$  where  $P_g = \beta P_{\text{tot}}$ ,  $P_m = (1 - \beta)P_{\text{tot}}$ ). NMGP go further and assume that the magnetic field is separately “assigned” to electrons and ions, and the ratio of gas to magnetic pressure in each component is the same. That implies that also some part of magnetic field energy is associated with the electron gas:

$$P_e = 1\beta n_e k T_e \quad U_e = [3(1 - \beta)\beta + a(T_e)] n_e k T_e \rho \quad (1)$$

where  $n_e$  is the electron concentration,  $T_e$  is the temperature of the electron gas,  $k$  is the Boltzmann constant, and  $U_e$  is the energy density associated with electrons per unit rest mass of the fluid with rest mass density  $\rho$ . The ratio of the energy density to the pressure for the electron component of the fluid  $a(T_e)$  is given as:

$$a(T_e) = 1\Theta_e [3K_3(1/\Theta_e) + K_1(1/\Theta_e)4K_3(1/\Theta_e) - 1] \quad (2)$$

In the above formula we use the dimensionless electron temperature  $\Theta_e = kT_e/m_e c^2$ , and  $K_i$  are the modified Bessel functions.

The term describing the advection of heat by electrons  $q_{\text{adv},e}$  is proportional to the entropy gradient along the streamlines, and can be expressed using the temperature and density gradients (NMGP):

$$q_{\text{adv},e} = n_e k T_e u^r [(3 - 3\beta\beta + a(T_e) + T_e da/dT_e) dT_e T_e dr - 1\beta p dp/dr] \quad (3)$$

where  $u^r$  is the radial component of the four velocity in the Boyer Lindquist coordinates. The equation of the thermal equilibrium for electrons has the form

$$q_{\text{ie}}^+ + q_{\text{vis,e}}^+ = q_{\text{adv,e}} + q_{\text{s,C}}^- + q_{\text{br,C}}^- \quad (4)$$

where  $q_{\text{ie}}^+$  is the rate of heating of electrons by Coulomb interactions with ions,  $q_{\text{vis,e}}^+$  is the rate of the direct heating of electrons by dissipative processes,  $q_{\text{s,C}}^-$  is the synchrotron, and  $q_{\text{br,C}}^-$  the bremsstrahlung cooling rate, both including Comptonization. We assume that the direct energy dissipation to the electron gas is a small fraction  $\delta$  of the total dissipation rate  $q_{\text{vis,e}}^+ = \delta q_{\text{vis}}^+$ . Methods of calculating terms  $q_{\text{ie}}^+$ ,  $q_{\text{vis}}^+$ ,  $q_{\text{s,C}}^-$ , and  $q_{\text{br,C}}^-$  are given in Papers I and II.

We find the distribution of electron temperature in the configuration iteratively solving the equation for thermal balance. Because the advection of heat by electron gas is now included in the equations, the conditions in any place in the disk depend on the conditions upstream. In our iterations we start from the outer layers of the configuration and follow the fluid inward. The temperature of the electrons in the whole configuration has an impact on the average optical depth, especially for soft photons. This influences the characteristic frequency of synchrotron selfabsorption, and hence the rate of cooling. The approach to this problem of non-locality has been described in Paper II. As our previous calculations show, the electron temperature in a given location does not depend strongly on the conditions around. Thus it is possible to obtain a selfconsistent electron temperature distribution after a few iterations, even if one starts from a primitive first approximation  $T_e(r, \theta) = \text{const}$ .

### 3. Results

We have calculated several ADAF models with parameters listed in Table 1. These parameters are: the mass of the black hole expressed in solar masses  $m = M_{\text{BH}}/M_{\odot}$ , the accretion rate in units of the critical accretion rate  $\dot{m} = \dot{M}/\dot{M}_{\text{crit}}$  (where  $\dot{M}_{\text{crit}} = L_{\text{Edd}}/c^2 = 1.4 \times 10^{17} m \text{ g s}^{-1}$ ) and parameters  $\beta$  and  $\delta$ . The black hole spin  $a$  takes three values: 0, 0.5 and 0.9 in each model. We have chosen only one value of the viscosity parameter,  $\alpha = 0.1$ , common for all models. We use gravitational radius  $r_g = GM/c^2$ , where  $G$  is the gravity constant and  $c$  is the speed of light. We have assumed that at the outer boundary of the flow  $r_{\text{out}} = 10^3 r_g$  the specific angular momentum is close to 95% of the Keplerian specific angular momentum ( $\ell \approx 0.95 \ell_K$ ). The radial component of the velocity is much smaller than the speed of sound at the boundary, so the flow is subsonic at the outer boundary. In Models 9 and 10 we have chosen the same values of  $m$ ,  $\dot{m}$  and  $\beta$  as in Paper II to examine the influence of the new heating and cooling rates in the thermal equilibrium equation (4) on the radiation spectra of the flow.

As in Paper II we solve the equations for thermal equilibrium (4) and the equation of state on the 2-dimensional grid in the  $(r, \theta)$  plane. The grid cells are spaced logarithmically in radius and linearly in polar angle. We use 25 values of radius

Table 1: Parameters of models.

Model	m	$\dot{m}$	$\beta$	$\delta$
1	$10^8$	$10^{-2}$	0.95	$10^{-3}$
2	$10^8$	$10^{-2}$	0.5	$10^{-3}$
3	$10^8$	$10^{-3}$	0.95	$10^{-3}$
4	$10^8$	$10^{-3}$	0.5	$10^{-3}$
5	$10^7$	$10^{-2}$	0.95	$10^{-3}$
6	$10^7$	$10^{-2}$	0.5	$10^{-3}$
7	$10^7$	$10^{-3}$	0.95	$10^{-3}$
8	$10^7$	$10^{-3}$	0.5	$10^{-3}$
9	$3.6 \times 10^7$	0.016	0.95	$10^{-3}$
10	$3.6 \times 10^7$	0.016	0.95	0

$\lg r \in [\lg r_h + 0.05; 3]$ , where  $r_h = (1 + \sqrt{1 - a^2})r_g$  is the radius of the black hole event horizon. The polar angle  $\theta$  (measured from the rotation axis) takes 19 values from  $0^\circ$  to  $90^\circ$  with  $\Delta\theta = 5^\circ$ . The radiation spectra of the flow are calculated in the same manner as in Paper II. Using Monte Carlo methods we have obtained Comptonized spectra of input synchrotron and bremsstrahlung photons in function of their frequency at infinity. We have also investigated the dependence of the observed flux of radiation on the inclination angle of the observer relative to the axis of rotation. The resulting spectra and bolometric fluxes presented in this paper are based on calculations including  $3 \times 10^5$  synchrotron and  $3 \times 10^5$  bremsstrahlung input photons and following about 3 - 5 times as many branches of photon trajectories in each case.

First, we examine the impact of the new terms in the thermal balance equation (the direct heating of electrons by dissipative processes  $q_{\text{vis,e}}^+$  and the advection of heat energy by electrons  $q_{\text{adv,e}}$ ) on the radial distribution of the electron temperature and radiation spectra of the flow. In the middle and right panels of Fig. 1 we compare the results obtained in Model 9 (electron advection and dissipation included), Model 10 (dissipation neglected) and the model from Paper II (both neglected). It is clearly seen that the direct energy dissipation to the electrons does not affect the energetic balance of the electron gas, so it can not influence the radiation spectrum. The spectra with advection by electrons and without it differ noticeably but not substantially.

In the left panel of Fig. 1 we show the radial dependence of the cooling and heating rates of electrons in Model 9. The advection of heat by electrons is the efficient cooling process in the outer part of the flow ( $\lg r \gtrsim 1.5$ ) and the efficient heating process in the inner part of the flow. It causes changes in the radial distribution of the electron temperature but not large and mostly in the outer region ( $\lg r \gtrsim 1.5$ ). The changes in the radiation spectra (especially in the slope of Comptonized spectra of synchrotron radiation) are also not big.

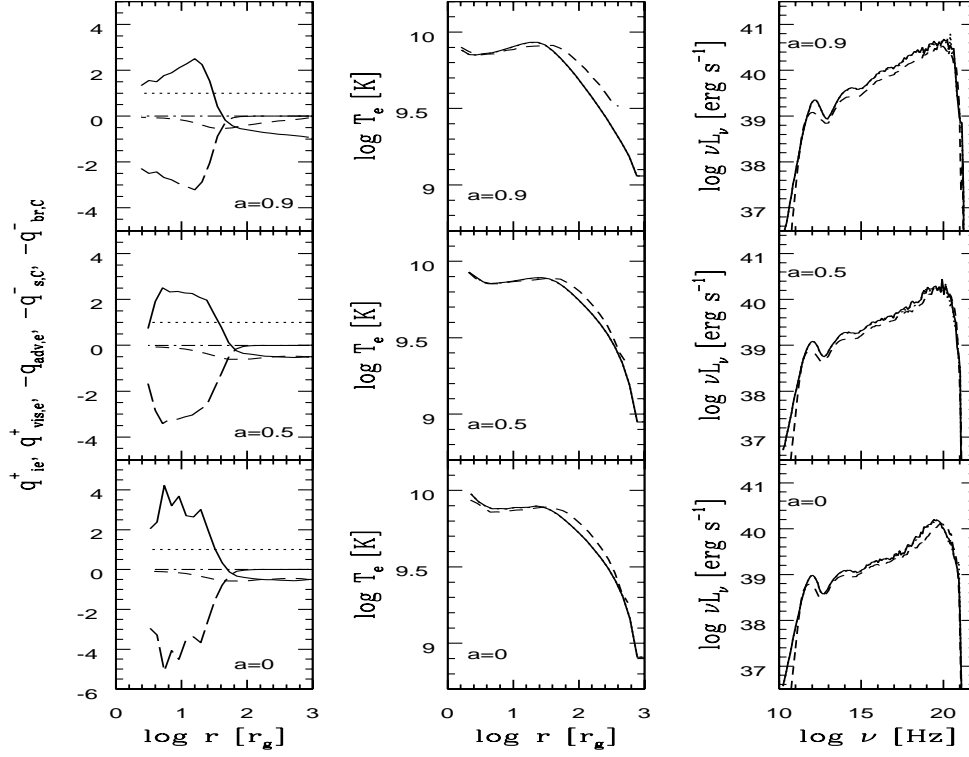


Figure 1: The influence of the direct electron heating and advection of heat by electrons on their temperature distribution and on the resulting spectra. For comparison we show the results for the models with parameters  $(m, \dot{m}, \beta) = (3.6 \times 10^7, 0.016, 0.95)$  of Paper II. **Left panel:** The relative importance of various heating (positive values) and cooling (negative values) processes at the equator for Model 9. The rate of electron heating by Coulomb interactions with ions  $q_{ie}^+$  is used for comparison and shown as dotted straight line at value 1. The rate of the direct heating by dissipative processes  $q_{vis,e}^+$  (dot-dashed), the term describing the advection of heat by electrons  $q_{adv,e}$  (solid), the synchrotron cooling rate including Comptonization  $q_{s,C}^-$  (long-dashed), and the bremsstrahlung cooling rate including Comptonization  $q_{br,C}^-$  (short-dashed) are shown as functions of radius in units of  $q_{ie}^+(r)$ . **Middle panel:** The radial dependence of the electron temperature at the equator for Model 9 (solid lines), Model 10 (dotted lines, covered with solid lines) and model described in Paper II (dashed lines). **Right panel:** The radiation spectra of ADAF for these cases. The three diagrams in each panel correspond to different values of the black hole spin, as indicated.

Figure 2 shows the effects of model parameters  $m$ ,  $\dot{m}$  and  $\beta$  on the radial distribution of the cooling and heating rates of electrons. We present the results for  $a=0.9$  only, because the influence of the black hole spin is not big. We see that also the black hole mass does not affect strongly the energetic balance of electrons. Much

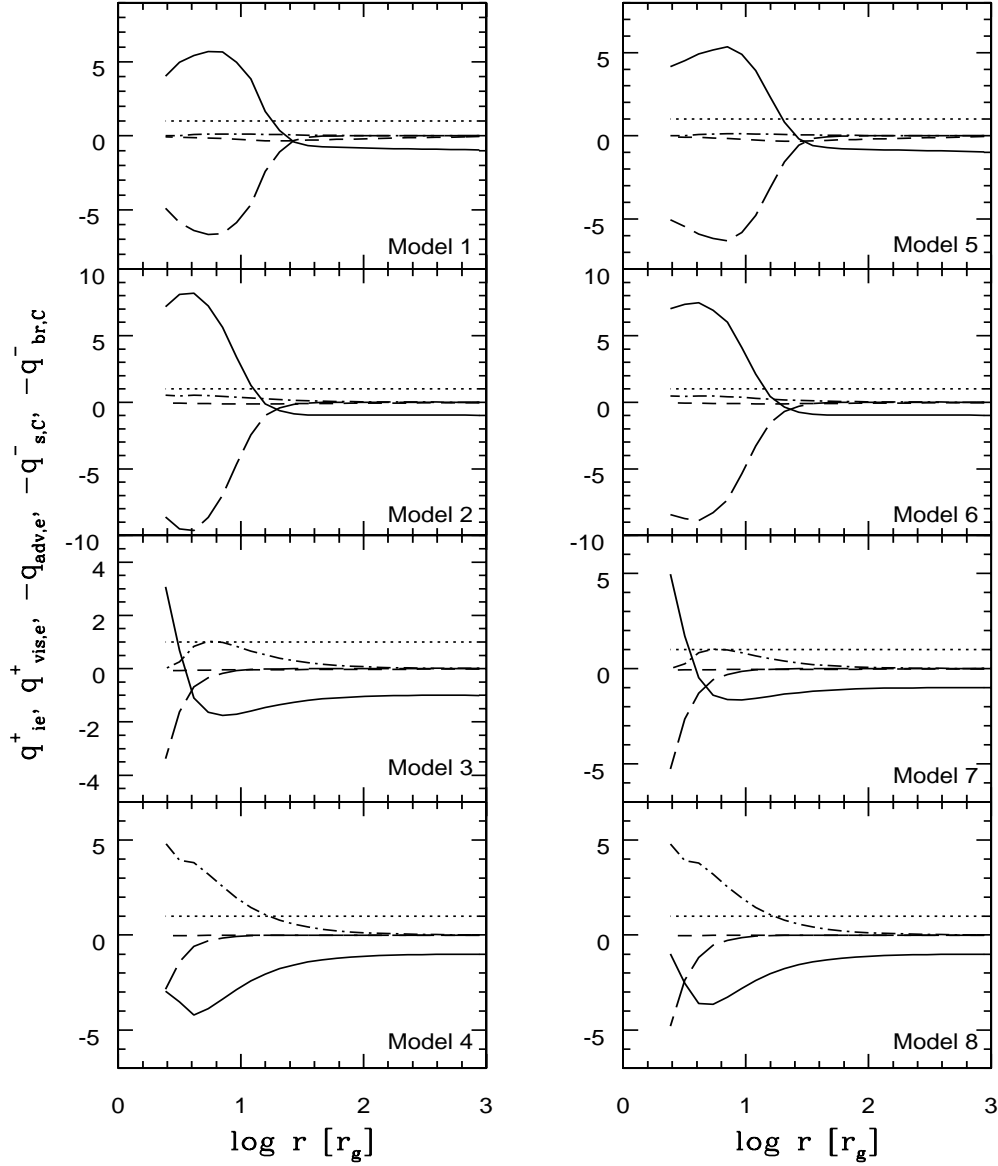


Figure 2: The same as in left panel of Fig. 1, but for Models 1-8.

more important are the accretion rate and parameter  $\beta$ . The smaller are  $\dot{m}$  and  $\beta$  (it means smaller density of the flow and higher density of the magnetic field in the plasma), the stronger is the influence of the direct energy dissipation to the electrons on their energetics. Simultaneously the radius at which advection by electrons becomes a heating process decreases. For  $\dot{m} = 10^{-3}$  and  $\beta = 0.5$  (Models 4 and 8), for example, there is no advective heating of the electrons – all the advectively transported heat is carried in under the black hole horizon. These effects cause

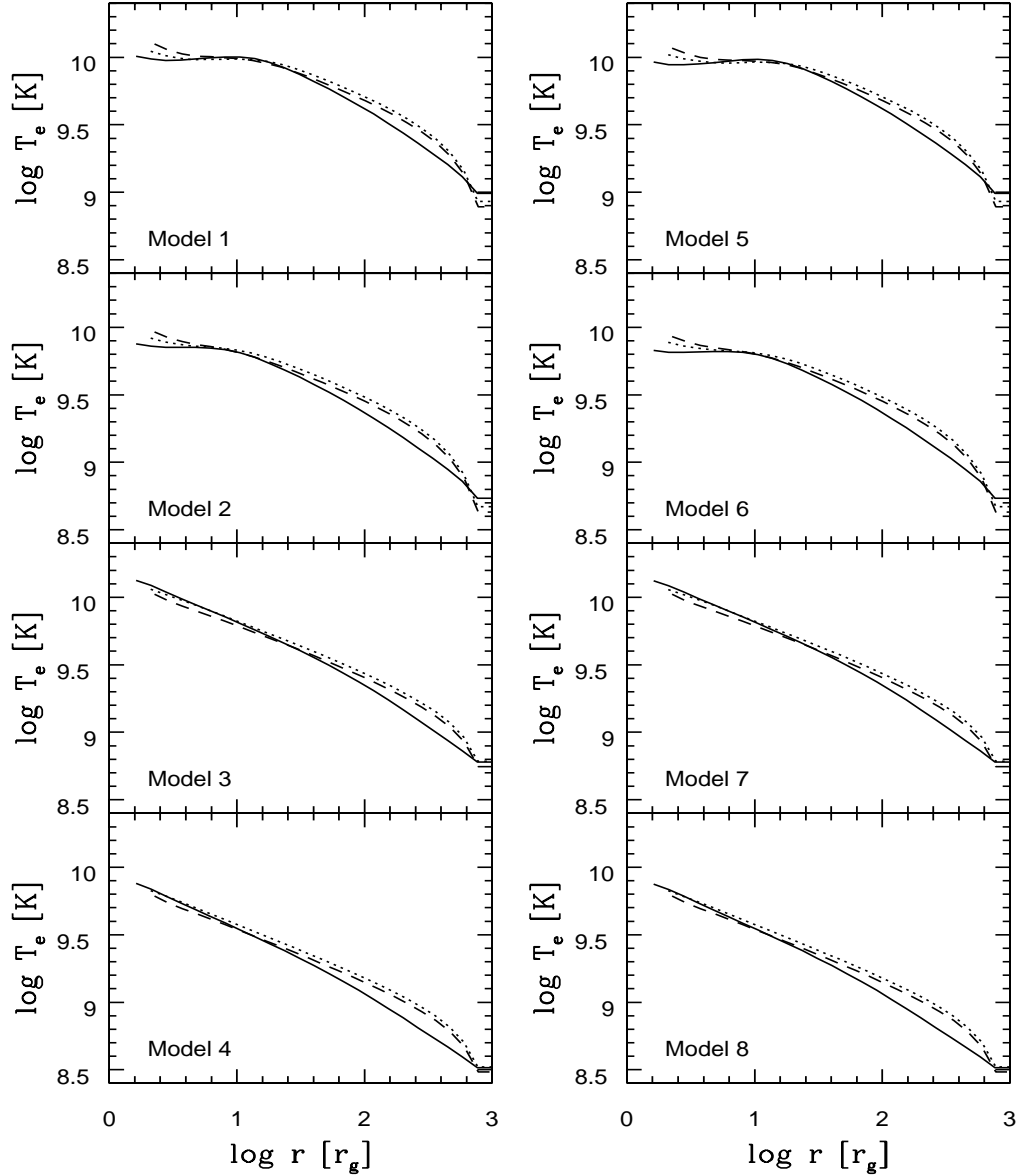


Figure 3: The radial dependence of the electron temperature at the equator for Models 1-8. The short-dashed, dotted and solid lines represent the cases with  $a=0, 0.5, 0.9$ , respectively.

the changes in radial distribution of the electron temperature in the flow, which is shown in Fig. 3. With decreasing  $\dot{m}$  and  $\beta$  the profile of the radial distribution of the electron temperature is more and more steep losing the characteristic flat nature for small radii. These results are in good agreement with results of Nakamura et al. (1997) and NMGP.

Finally, in Fig. 4 and Fig. 5 we show the influence of the model parameters



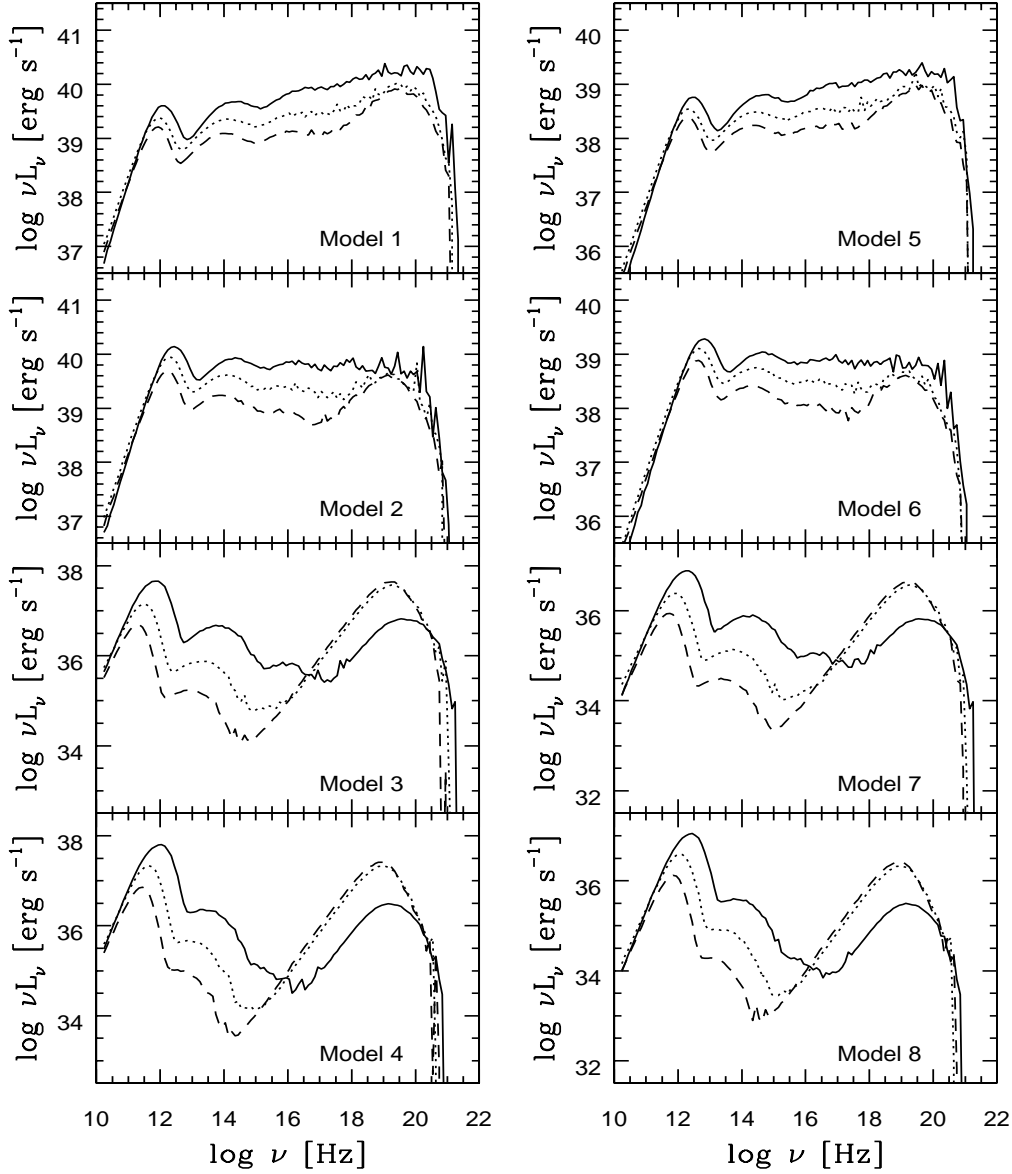


Figure 4: The radiation spectra of ADAF for Models 1-8. The three cases of the Kerr parameter  $a$  are represented by the same types of lines as in the Fig. 3.

on the radiation spectra  $\nu L_\nu$  and on the observer - inclination dependence of the bolometric flux measured at infinity,  $L(i)$ . There are three main components of the radiation spectra of ADAFs which dominate in the  $\lg(\nu)$  vs.  $\lg(\nu L_\nu)$  plot: the synchrotron peak (radio energies), the bremsstrahlung peak (X-ray and soft  $\gamma$ -ray energies) and the Comptonized spectra of the synchrotron radiation between them (sometimes this component covers the bremsstrahlung peak). The shapes and

relative positions of the synchrotron and bremsstrahlung peaks in the plot, as well as the slope of the Comptonized spectrum (expressed by power law index  $\Gamma$ , where  $L_\nu \sim \nu^{-\Gamma}$ ) depend on the distribution of the electron temperature and density in the flow, so they depend on the model parameters.

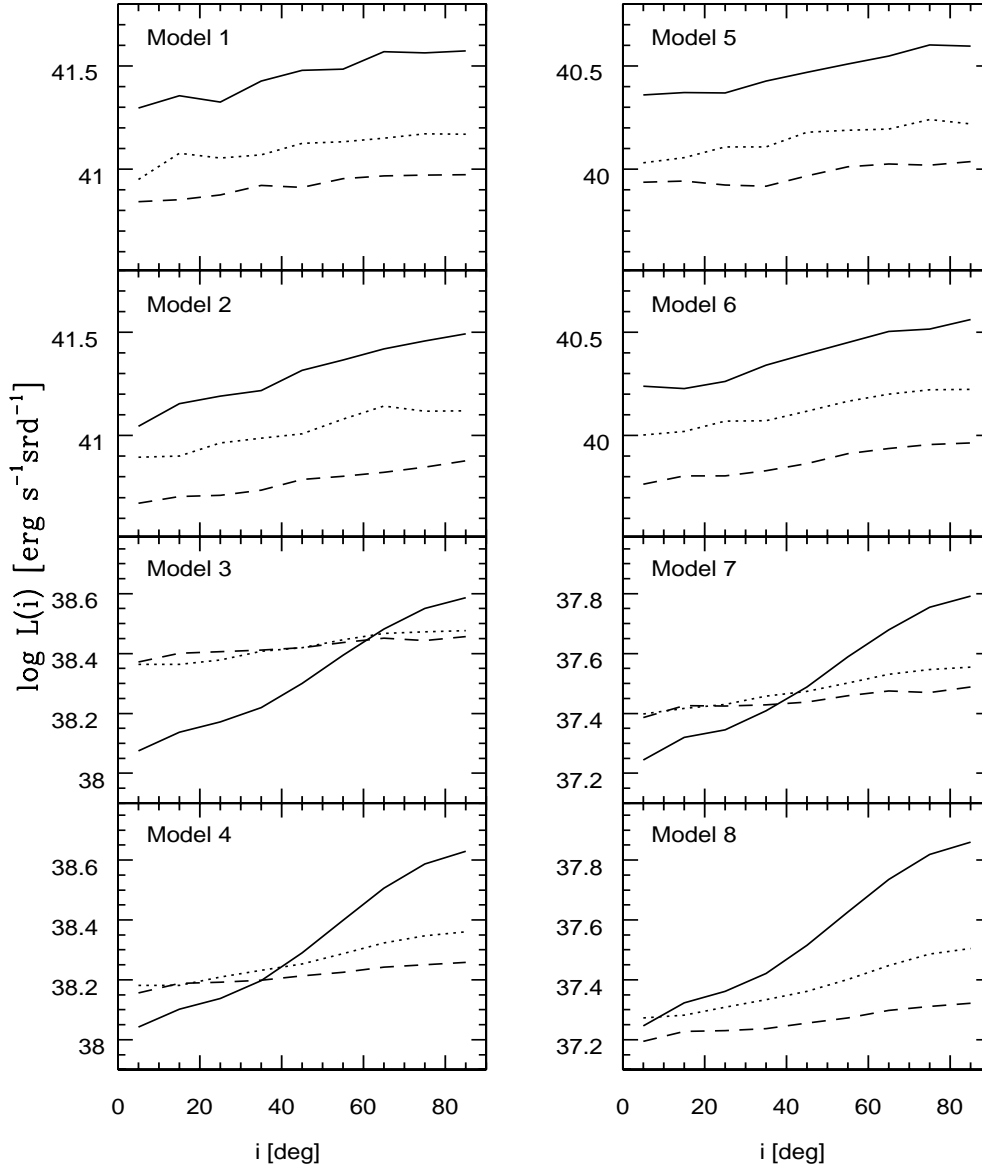


Figure 5: The dependence of the observed total bolometric flux from the ADAF on the observer inclination relative to the axis of rotation for Models 1-8. The three cases of the black hole spin  $a$  are represented by the same types of lines as in the Fig. 3.

There is very weak dependence of the radiation spectra and luminosity anisotropy on the black hole mass. The total bolometric luminosity, however, is directly proportional to  $m$ . With decreasing  $\beta$  the synchrotron peak becomes higher, the power law index of the Comptonized spectra becomes smaller and  $L(i)$  slightly steeper. The greatest influence on radiation spectra and bolometric flux has the accretion rate. This topic, however, has been examined very well in many papers devoted to ADAFs and the dependencies of bolometric luminosity of each component of the ADAFs spectrum on  $\dot{m}$  is rather obvious. The most interesting result of our investigations in this paper (and Paper II) is the influence of the black hole angular momentum on radiation spectra. With increasing  $a$  the index  $\Gamma$  becomes lower which corresponds to flatter  $L_\nu \sim \nu^{-\Gamma}$  spectrum with relatively more high energy photons. The total luminosity becomes higher and the anisotropy of the source is more pronounced, which corresponds to the steeper dependence of the observed luminosity on the inclination angle,  $L(i)$ . The anisotropy is not very big. In most cases the ratio of the luminosity observed at the equator to the luminosity observed on the rotation axis  $L(90^\circ)/L(0^\circ) \in [1.1; 2]$ . The exceptions are the models with  $a = 0.9$  and  $\dot{m} = 10^{-3}$ , where this ratio reaches values  $\sim 4$ .

#### 4. Discussion and conclusions

In this paper we have used the dynamical models of ADAFs obtained with the methods of Papers I and II. We assume that the influence of the cooling processes on the dynamics of the flow can be neglected, since the advection of heat dominates. This assumption allows us to solve the problem of heat and radiation transport separately. We do not consider the possibility of matter outflow from the inner parts of the disk. This scenario, called Advection Dominated Inflow - Outflow Solutions, has been put forward by Blandford and Begelman (1999). Following the discussion presented by Paczyński (1998) based on his semi-analytic model of the flow and also the physical and 2D numerical analysis of the problem by Abramowicz, Lasota and Igumenshchev (2000) we think that models neglecting the outflows are selfconsistent.

The outer boundary conditions in our models resemble the *Preheated* ADAFs of Park and Ostriker (1999; 2000) in the sense that the thermal energy of the fluid at the outer edge of the disk is a substantial part of its virial energy. The problem of transition from Keplerian disk to advection dominated flow has not been solved yet so the outer boundary condition can not be introduced in a "natural" way. Other aspects of our method are different: we use solutions of height averaged equations for the disk structure instead of self-similar solutions of Narayan and Yi (1995) employed by Park and Ostriker (2000). To get the two dimensional distribution of the fluid density we use the approach of Paper II. We assume the specific angular momentum and the radial component of the velocity to be constant on  $r = \text{const}$  "spheres". This is sufficient to calculate the density distribution on the spheres. In

our approach the empty funnels near the rotation axis arise naturally due to the existence of centrifugal potential barrier. The funnels are not conical and their opening angles vary from  $\sim 30^\circ$  at small radii to  $\sim 5^\circ$  at larger distances from the black hole. These results are in agreement with Park and Ostriker (2000) calculations assuming preheating of ADAFs.

We have not explored the models for as large a range of accretion rates as has been done by Park and Ostriker (2000), so we can not comment on the limits on accretion rate  $\dot{m}$  for which the models remain selfconsistent and belong to the class of (Preheated) ADAFs. In our calculations we have not met any problems with energy balance equation. We think that conclusions referring to the necessity of including matter outflows and/or preheating in modeling ADAFs must await a fully 2D treatment of the combined dynamical and radiative transfer equations.

In this paper we have changed our equation for the thermal energy balance of Paper II including the direct heating of electrons by dissipation and taking into account the advection of heat by electron gas (NMGPG; Nakamura et al. 1997). The direct comparison of the models including and not including the changes shows, that the heating of electrons by dissipation (at the rate  $10^3$  times lower than for ions) has practically no influence on the electron temperature distribution and does not change the resulting radiation spectra of the flows. On the contrary, the advection of heat by electrons substantially changes the thermal structure of the flow. The advection plays the role of cooling process in the outer regions of the disks, where most of the energy delivered to the electrons by Coulomb interactions is stored and transported inward. In the inner parts of the flow some part of this energy is radiated, especially in high accretion rate cases ( $\dot{m} \gtrsim 10^{-2}$ ).

We have calculated a larger family of models using slightly improved methods as compared with Paper II. Our calculations include all relativistic effects in light propagation and scattering and employ extensively Monte Carlo approach. Our conclusion from Paper II remains valid: for other parameters kept constant, the spectra of more rapidly rotating black holes are harder. The Doppler boost of photons, which happen to be scattered many times, is probably one of the factors, but more important factor is the systematic difference between density distribution in the inner parts of the flow depending on the angular momentum of the hole. For spinning holes the sonic radius is smaller. Inside this radius the flow is close to the free fall, but outside it the pressure gradients partially control and slow down the radial velocity of the flow. At given radius the velocity of inflow toward the rapidly rotating black hole is slower than the velocity toward a Schwarzschild black hole, because the distance remaining to the sonic point is larger in this case. If the accretion rates in both cases are the same, the density must be higher in the case of rotating hole. Higher density explains relatively higher rate of synchrotron radiation and a higher probability of scattering. Such effects are seen in our spectra: the first synchrotron peaks have heights monotonically increasing with black hole spin  $a$  and the scattered (high energy) photons are more abundant.

All our models are anisotropic sources of radiation and equatorial observers are preferred in all cases. The effect is not as strong as described in Paper I, but not negligible. The largest anisotropy is present in low accretion rate ( $\dot{m} = 10^{-3}$ ) ADAFs around Kerr ( $a = 0.9$ ) black holes. It must be caused by the relativistic effects in light scattering and propagation (mostly the Doppler effect).

**Acknowledgements.** This work was supported in part by the Polish State Committee for Scientific Research grants 2-P03D-012-16 and 2-P03D-013-16

## REFERENCES

- Abramowicz, M.A., Chen, X., Granath, M., and Lasota, J.-P. 1996, *Astrophys. J.*, **471**, 762.  
 Abramowicz, M.A., Lanza A., and Percival M.J. 1997, *Astrophys. J.*, **479**, 179.  
 Abramowicz, M.A., Lasota, J.-P., and Igumenshchev, I.V. 2000, *astro-ph/0001479*.  
 Bardeen, J.M. 1973, *In: Black Holes*, ed. C. DeWitt and B.S. DeWitt (Gordon & Breach, New York), p. 215.  
 Blandford, R.D., and Begelman, M.C. 1999, *MNRAS*, **303**, L1.  
 Gammie, C.F., and Popham, R.G. 1998, *Astrophys. J.*, **498**, 313.  
 Jaroszyński, M., and Kurpiewski, A. 1997, *Astron. Astrophys.*, **326**, 419 (Paper I).  
 Kato, S., Fukue, J., and Mineshige, S. 1998, *Black Hole Accretion Disks*, (Kyoto University Press, Kyoto).  
 Kurpiewski, A., and Jaroszyński, M. 1999, *Astron. Astrophys.*, **346**, 713 (Paper II).  
 Lasota, J.-P. 1994, *In: Theory of the Accretion Disks 2*, ed. W.J. Duschl, J. Frank, F. Meyer, E. Meyer-Hoffmeister and W.M. Tscharnutter (Kluwer Academic Publishers, Dordrecht), p. 341.  
 Lasota, J.-P. 1999, *Phys. Reports*, **311**, 247.  
 Nakamura, K.E., Kusunose, M., Matsumoto, R., and Kato, S. 1997, *P.A.S.J.*, **49**, 503.  
 Narayan, R., and Yi, I. 1994, *Astrophys. J.*, **428**, L13.  
 Narayan, R., and Yi, I. 1995, *Astrophys. J.*, **444**, 231.  
 Narayan, R., Mahadevan, R., Grindlay, J.E., Popham, R.G., and Gammie, Ch. 1998, *Astrophys. J.*, **492**, 554 (NMGP).  
 Narayan, R., Mahadevan, R., and Quataert, E. 1998, *In: The Theory of Black Hole Accretion Disks*, ed. M.A. Abramowicz, G. Björnsson and J. Pringle (Cambridge University Press, Cambridge).  
 Paczyński, B. 1998, *Acta Astron.*, **48**, 667.  
 Park, M.-G., and Ostriker, J.P. 1999, *Astrophys. J.*, **527**, 247.  
 Park, M.-G., and Ostriker, J.P. 2000, *astro-ph/0001446*.  
 Peitz, J., and Appl, S. 1997, *MNRAS*, **286**, 681.  
 Popham, R.G., and Gammie, C.F. 1998, *Astrophys. J.*, **504**, 419.  
 Svensson, R. 1998, *In: Theory of Black Hole Accretion Disks*, ed. M.A. Abramowicz, G. Björnsson and J.E. Pringle (Cambridge University Press).  
 Yi, I. 1999, *In: Astrophysical Discs, ASP Conf. Series 160, astro-ph/9905215*.